RESEARCH ARTICLE

3D-bioprinted Recombination Structure of Hertwig's Epithelial Root Sheath Cells and Dental Papilla Cells for Alveolar Bone Regeneration

Huilin Tang[1,2,3], Fei Bi[1,2,3], Guoqing Chen[4], Shuning Zhang[1,2,3], Yibing Huang[1,2,3], Jiahao Chen[1,2,3], Li Xie[5,6], Xiangchen Qiao[7], Weihua Guo[1,2,3]*

[1]State Key Laboratory of Oral Disease, West China Hospital of Stomatology, Sichuan University, Chengdu, China
[2]National Clinical Research Center for Oral Diseases, West China Hospital of Stomatology, Sichuan University, Chengdu, China
[3]Department of Pediatric Dentistry, West China School of Stomatology, Sichuan University, Chengdu, China
[4]Department of Human Anatomy, School of Medicine, University of Electronic Science and Technology of China, Chengdu, China
[5]National Engineering Laboratory for Oral Regenerative Medicine, West China Hospital of Stomatology, Sichuan University, Chengdu, China
[6]Engineering Research Center of Oral Translational Medicine, Ministry of Education, State Key Laboratory of Oral Diseases, National Clinical Research Center for Oral Diseases, West China Hospital of Stomatology, Sichuan University, Chengdu, China
[7]Chengdu Renjitiancheng Biotechnology Limited Corporation, Chengdu, China

Abstract: Three-dimensional (3D) bioprinting is an emerging method for tissue regeneration. However, promoting the epithelial-mesenchymal interaction (EMI), while maintaining the characteristics of epithelial cells has always been a challenge in tissue engineering. Since EMI acts as a critical factor in bone regeneration, this study aims to promote EMI by recombining epithelial and mesenchymal cells through 3D bioprinting. Hertwig's epithelial root sheath (HERS) is a transient structure appeared in the process of tooth root formation. Its epithelial characteristics are easy to attenuate under appropriate culture environment. We recombined HERS cells and dental papilla cells (DPCs) through 3D bioprinting to simulate the micro-environment of cell-cell interaction *in vivo*. HERS cells and DPCs were mixed with gelatin methacrylate (GelMA) separately to prepare bio-inks for bioprinting. The cells/GelMA constructs were transplanted into the alveolar socket of Sprague-Dawley rats and then observed for 8 weeks. Hematoxylin and eosin staining, Masson staining, and immunohistochemical analysis showed that dimensional cultural pattern provided ideal environment for HERS cells and DPCs to generate mineralization texture and promote alveolar bone regeneration through their interactions. 3D bioprinting technology provides a new way for the co-culture of HERS cells and DPCs and this study is inspiring for future research on EMI model.

Keywords: Epithelial-mesenchymal interaction; 3D bioprinting; Hertwig's epithelial root sheath cell; Alveolar bone regeneration

***Correspondence to:** Weihua Guo, Department of Pedodontics, West China College of Stomatology, Sichuan University, No.14, 3rd Section, Renmin South Road, Chengdu 610041, PR China; guoweihua943019@163.com

Received: February 1, 2022; **Accepted:** April 20, 2022; **Published Online:** June 10, 2022

(This article belongs to the *Special Issue: 3D Bioprinting with Photocurable Bioinks*)

Citation: Tang H, Bi F, Chen G, *et al*., 2022, 3D-bioprinted Recombination Structure of Hertwig's Epithelial Root Sheath Cells and Dental Papilla Cells for Alveolar Bone Regeneration. *Int J Bioprint*, 8(3):512. http://doi.org/10.18063/ijb.v8i3.512

1. Introduction

The development of tooth is a complicated process during which the epithelial cells interact with the mesenchymal cells[1]. Strategies to accomplish tooth regeneration by tissue engineering have always been an academic focus in recent years[2-4]. Researchers have successfully isolated

epithelial cells and mesenchymal cells derived from embryos to rebuild bioengineered tooth germ[5]. Although they generated a tooth with complete anatomical structure, the embryonic stem cells confined their widespread applications in clinical practice. Besides, the bioengineered tooth was irregular in both morphology and quantitative terms, and epithelial-mesenchymal interaction (EMI) was also in no small measure overlooked as the *in vitro* experiment was conducted with two-dimensional cell culture. To optimize the EMI process, other researchers tried building a biomimetic 3D tooth bud model by combining cell patch with dental epithelial and mesenchymal cells loaded with gelatin methacrylate (GelMA) hydrogel[6,7].

With respect to the foregoing, it could be fraught with difficulties to realize the regeneration of tooth with both crown and roots for now. Tooth root regeneration seems more feasible than whole tooth regeneration in clinical view. During tooth development, when the formation of crown is nearly complete, the root begins to develop. The inner and outer enamel epithelia proliferate around cervical loop and form a bilayered epithelial sheath known as Hertwig's epithelial root sheath (HERS). Considering that the inner cells of HERS initiate the differentiation of odontoblast to form root dentin, HERS is indispensable to root development. For instance, if the continuity of HERS were damaged, it could not induce dental papilla cells (DPCs) to differentiate into odontoblasts, which could result in dentin defects. In addition, if the epithelial root sheath failed to break at specific time and adhered to the surface of the root dentin, the dental follicle cells could not differentiate into cementoblasts to form cementum[8,9]. In a previous study, we found that the HERS spheroids could promote HERS cell proliferation and optimize its biological function[10]. The experiment verified the capability of HERS spheroids in the induction of DPCs differentiation by mixing HERS spheroids with DPCs, but the interaction between cells was also limited to some extent. The issue that needs to be addressed is to maximally maintain the epithelial characteristics of HERS and thereby inducing DPCs to form new mineralized tissue.

Three-dimensional (3D) bioprinting is the technology using a bioprinter to produce the pre-designed 3D structure made of different kinds of biomaterials and transit them to biologically active tissues or organs[11]. This cutting-edge technology enables the realization of new ideas for tissue engineering and shows great potential in biomedical applications due to its high precision and high throughout[12,13]. Fabricated 3D fibrous scaffolds exhibited excellent ability to guide cell to arrange along the fiber axis[14]. In addition, "time" was incorporated into 3D bioprinting as the fourth dimension[15]. In 4D bioprinting, the functionality of printed construct would change along with time under external stimulus, which might serve as a useful tool for bio-fabrication in stimulating the biological function changes *in vivo*[16,17]. GelMA containing the characteristics of natural and synthetic biological materials, can be cross-linked and solidified into gel by ultraviolet light under the action of photoinitiator[18]. Besides, GelMA has excellent biocompatibility, biodegradability, cell response characteristics, and the 3D structure suitable for cell growth and differentiation[19]. In recent years, GelMA has been widely used in 3D cell culture, tissue engineering and 3D bioprinting[20-23]. Stem cells and extracellular matrix were encapsulated in GelMA and poly(ethylene glycol) dimethacrylate composite hydrogel for alveolar bone repair[24]. 3D-printed cell/GelMA constructs could mimic the micro-environment *in vivo*. Meanwhile, it provides excellent conditions for cellular activity and optimized cell-cell interactions[25]. Therefore, according to the spatial relationship between HERS cells and DPCs during tooth germ development, we designed structural model of these two kinds of cells and prepared two bio-inks using GelMA hydrogel for 3D bioprinting (**Figure 1**). An alveolar bone defect model was applied to test the osteogenesis effects of 3D printed co-culture constructs. This study puts forward a new method to recombine HERS cells and DPCs through 3D bioprinting, which could contribute to the investigation of EMI research in the future.

2. Materials and methods

2.1. Ethics statement

Animals were purchased from Dashuo Experimental Animal Co. Ltd. (Chengdu, China). All animal experiments in this study were approved by the Research Ethics Committee of West China Hospital of Stomatology, Sichuan University (permit no. WCHSIRB-D-2021-551).

2.2. Cell isolation and culture

Primary HERS cells and DPCs were isolated from the first molar germ in the maxilla and mandible of 8-day-postnatal Sprague-Dawley (SD) rats (**Figure S1**), and the specific method was mentioned in the previous studies[26,27]. After being sheared to fragments, the tissue was digested by type I collagenase and dispase (Sigma-Aldrich, USA) solution at 37°C for 10–20 min.

HERS cells were cultured in epithelial cell medium (ScienCell, USA) containing 1% epithelial cell growth supplement, 2% fetal bovine serum, and 1% penicillin/streptomycin solution. Mixed with mesenchymal cells, HERS cells in passage 0 were treated with 0.25% trypsin-EDTA (Gibco, USA) for 2–3 minutes, then purified HERS cells were obtained after 2–3 times of differential digestion. The adherent HERS cells were processed into cell suspensions under the treatment of TrypLE Express Enzyme (Thermo Scientific, USA) for 10–15 min. DPCs were cultured in alpha-minimum essential medium

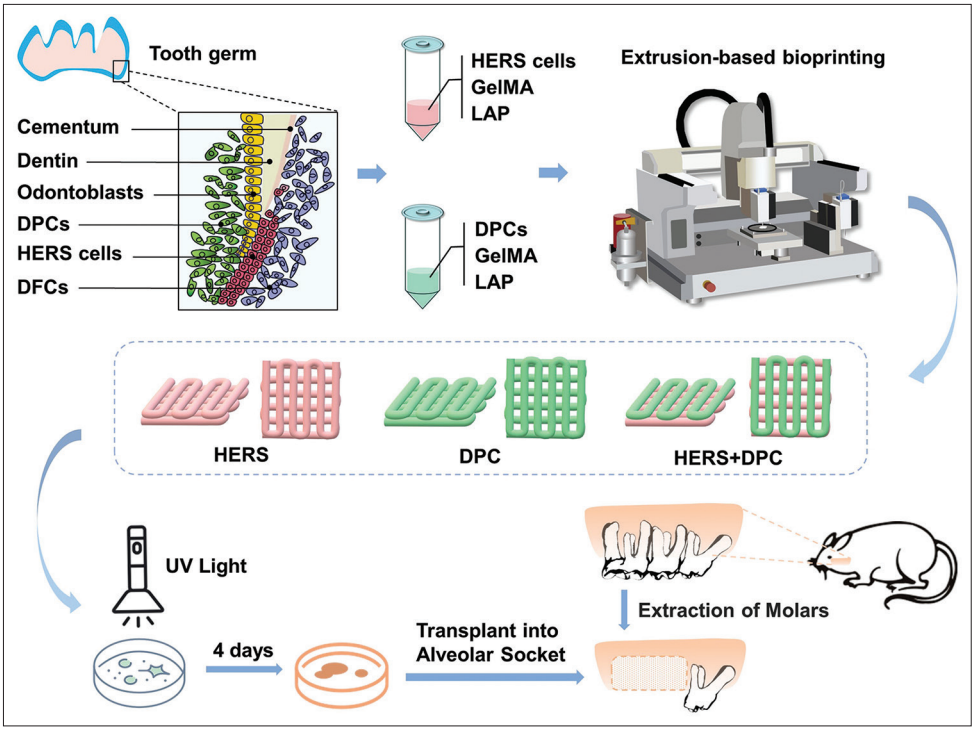

Figure 1. Fabrication, culture, and transplantation of printed constructs. Schematic diagram of 3D bioprinting and transplantation of constructs. DPCs: Dental papilla cells, GelMA: Gelatin methacrylate, HERS: Hertwig's epithelial root sheath, LAP: lithium phenyl-2, 4, 6-trimethylbenzoylphosphinate, UV light: Ultraviolet light.

(Gibco, USA) supplemented with 10% fetal bovine serum (Gibco, USA) and 1% penicillin/streptomycin solution (Solarbio, CHN). All cells were cultured in cell incubator with 5% CO_2 at 37°C and medium was changed every 2 days.

2.3. Immunofluorescence staining

The immunofluorescence staining procedures were carried out as previously described[26,28,29]. Antibodies used in this work include mouse anti-CK14 (1:200, MAB3232, Millipore), mouse anti-vimentin (1:200, sc-6260, Santa Cruz Biotechnology), and Alexa FluoR 488 Goat anti Mouse (1:500, A11001, Invitrogen). All samples were observed under confocal microscope (Olympus FV1200, Japan).

2.4. Bioink preparation

The process of bioink preparation was performed according to the manufacturer's instructions. The first step was to prepare the 0.25% (w/v) standard solution of lithium phenyl-2, 4, 6-trimethylbenzoylphosphinate (LAP), which served as a photoinitiator. The LAP was dissolved in phosphate buffered saline at 40–50°C for 15 min. Then lyophilized GelMA (GM-60, EFL, China) was dissolved in LAP solution at 37°C for 30 min and 10% (w/v) GelMA solution was filtered through 0.22 μm sterile filter. At last, cells were suspended by GelMA solution at a density of approximately 1×10^6 cells/mL on the basis of manufacturer's recommendation. HERS-laded bioink and DPCs-laden bioink were prepared separately for 3D bioprinting.

2.5. 3D bioprinting

The 3D epithelial-mesenchymal model was designed and resized to an 8.0 × 8.0 × 1.5 mm^3 cuboid, then exported into a STereoLithography file by Maya 2016 (Autodesk, USA). The 3D bioprinting was carried out by 4th Generation 3D-Bioplotter® Developer Series (EnvisionTEC, Germany), which was designed for the field of tissue engineering[30,31]. HERS-DPCs constructs were printed with two kinds of bioinks - each layer of HERS cells followed by two layers of DPCs. In other words, the ratio of two cells is 1:2, which was the same as in our previous research[10]. In this study, we used 27-gauge syringe needle, and the related printing parameters were set as follows: (i) pneumatic pressure: 0.8–1.1 bar; (ii) moving speed: 9–11 mm/s; (iii) temperature of print head: 25–27°C; (iv) temperature of platform: 15°C; and (v) distance between lines: 0.8 mm. Supplemented with culture medium after printing, the constructs were solidified with 405 nm light-curing portable source (EFL-LS-1601-405, EFL, China) for 30 s[25,32]. To evaluate the function of HERS-DPCs construct in osteogenesis, HERS cells alone construct and DPCs alone construct were bioprinted

according to the same model and parameters as control groups. All constructs were cultured for 4 days *in vitro* before implantation experiments.

2.6. Live/dead cell viability assay

The viability of HERS or DPCs cells encapsulated in GelMA hydrogel was tested by Live/Dead Viability/ Cytotoxicity Assay Kit for Animal Cells (KeyGEN, China) after 1, 4, and 7 days of incubation according to the manufacturer's instructions (n = 4). Live and dead cells were observed under laser scanning confocal microscope. The quantity of cells was counted through Image J software and the cell viability was quantified by calculating the proportion of living cells among all cells.

2.7. Cell labeling

Vybrant™ DiI and DiO cell-labeling solution (Thermo Scientific, USA) are commonly used cell tracers in cell-cell fusion, cellular adhesion, and migration research due to their low cytotoxicity and high stability. To investigate the interaction between HERS cells and DPCs loaded in GelMA, the two kinds of cells were dyed by DiI and DiO solutions separately according to the experimental protocols. First, we added the cell-labeling solution into serum-free alpha-minimum essential medium with the concentration of 5 μL/mL. Then cells were suspended by the working solution at a density of 1×10^6/mL and incubated for 15–20 min at 37°C. Finally, we resuspended cells in warm medium after the treatment of centrifugation at 1200 rpm for 5 min and repeated the procedure twice before viewing the cells under fluorescence microscope (Olympus, IX73, Japan).

2.8. Microscopic evaluation of constructs

GelMA scaffold was dehydrated by gradient alcohol to remove its aqueous phase. Then the scaffold was inspected under a scanning electron microscopy (SEM, Inspect F, FEI, USA) for microscopic observation.

2.9. Quantitative measurements of cell number and cell confluence

Cell convergence, the percentage of cell area in culture dish, was one of the main parameters in cell culture *in vitro* and usually used to assess cell proliferation[33,34]. In this study, we counted the cell number and cell confluence by Image J software (n = 4).

2.10. Alveolar socket transplantation in SD rats

8-week-old female SD rats (210–240 g) were used for alveolar socket transplantation experiment (n = 4). The experimental groups were designed as blank, DPCs (3D bioprinting), HERS (3D bioprinting), HERS+DPCs (3D bioprinting), and HERS+DPCs (mixed). The last group mixed HERS cells and DPCs at a ratio of 1:2 in GelMA solution without the process of 3D bioprinting. We extracted the first and the second right maxillary molars, and then prepared the alveolar socket into a $1.0 \times 2.0 \times 1.5$ mm^3 bone defect with a dental implant machine. No implant was used to fill the bone defect in the blank group while the four other groups implanted constructs matching the alveolar socket defect before suture. The digital X-ray films were taken before and after surgery. After 8 weeks, samples were collected and treated with 4% paraformaldehyde for 24 h, then decalcified with 10% ethylenediaminetetraacetic acid for 7 weeks. All specimens were embedded with paraffin for further analysis.

2.11. Histological and immunohistochemical staining

5 μm thick tissue sections were prepared for hematoxylin and eosin, Masson and immunohistochemical staining. All samples were treated in accordance with manufacturer's recommended protocols. Primary antibodies used in this work consisted of COL-I (1:200, ab270993, Abcam), OCN (1:500, ab93876, Abcam), RUNX-2 (1:500, ab76956, Abcam), and DSPP (1:500, 508413, Zen Bioscience). Briefly, specimens were deparaffined and hydrated by dimethylbenzene and ethanol, then permeabilized with 0.1% Triton X-100, treated with citrate antigen retrieval solution and blocked with 10% goat serum before incubated with primary antibodies in a moist chamber overnight at 4°C. After incubating secondary antibodies for 1–2 h at 37°C, DAB kit (Gene Tech, China) was used as a coloration solution and all slices were observed under light microscope (BX43F Olympus, Japan).

2.12. Statistical analysis

All statistical analyses were performed using SPSS 24.0 (SPSS Inc., Chicago, IL, USA). Student's t-test was used to compare the differences between two groups and one-way analysis of variance was performed to assess the discrepancies between multiple groups. $P < 0.05$ was considered statistically significant.

3. Results

3.1. Immunofluorescence measurements

The primary HERS cells grown in clusters with a cobblestone appearance under light microscope (**Figure 2A, a**). HERS cells expressed both epithelial cell marker CK14 and mesenchymal cell marker Vimentin, which were identified by immunofluorescence assay, indicating that they had the properties of epithelial and mesenchymal cells at the same time (**Figure 2A, b and** c).

3.2. Viability of the cells encapsulated in GelMA

The cell viability of HERS cells (**Figure 2B**) and DPCs (**Figure S2**) was evaluated by Live/Dead assays after

culturing for 1, 4, and 7 days. According to the statistical results (**Figure 2C**), the cells encapsulated in GelMA showed high viability (all over 80% on days 1, 4, and 7) and GelMA was proved biocompatible in 3D bioprinting.

3.3. HERS-DPCs interaction

To observe the interaction of HERS cells and DPCs in the 3D-printed GelMA scaffold *in vitro*, HERS cells were marked red and DPCs were marked green (**Figure 3A**). Next, we recorded the confocal images on day 0, day 3, and day 8. The results indicate that HERS cells and DPCs migrated to each other along the scaffold on day 8 (**Figure 3B and Figure S3**). The corresponding 3D videos of printed constructs were shown in **Figures S4-S6** and the graph schema showed the migration of the two kinds of cells (**Figure 3C**).

3.4. Microscopic observation of printed construct

The staggered grid structure of GelMA hydrogel scaffold was observed under optical and scanning electron microscopy (**Figure 4A-C**). Besides, cells crawled out from the scaffold (**Figure 4C, red arrow**) and proliferated since day 3. To evaluate the cells proliferation, cell number and cell confluence were calculated (**Figure 4D and E**). The number and confluence of cells increased significantly, indicating rapid cell proliferation at this stage.

3.5. Alveolar socket transplantation in SD rats

In the process of alveolar socket transplantation in SD rats, we first exposed the right posterior area of maxillary bone clearly (**Figure 4F, a**) and took a digital X-ray film before tooth extraction (**Figure 4G, a**). Then the first and second molars were extracted completely (**Figure 4F, b and c**) before mechanical preparation of the alveolar bone defect (**Figure 4F, d**). After transplanting the constructs, the oral mucosa and skin were tightened with layered sutures (**Figure 4F, e and f**). At last, a digital X-ray film was taken after operation (**Figure 4G, b**).

3.6. Histological and immunohistochemical analysis of transplantation *in vivo*

The HE and Masson staining marked plenty of newly formed collagen fiber in the operation area of all groups (**Figure 5**). The blank group, compared to other groups,

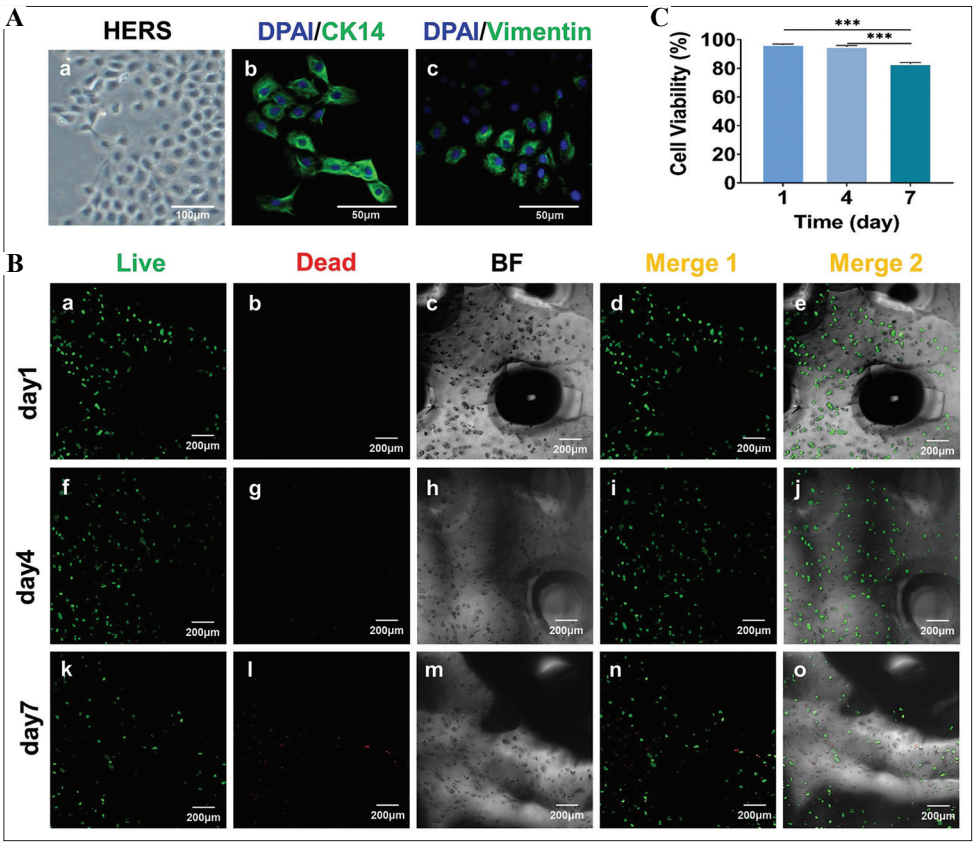

Figure 2. Isolation, culture, identification, and viability of HERS cells. (A) The isolation, culture, and identification of primary HERS cells. HERS cells expressed both epithelial marker CK14 and mesenchymal marker vimentin. (B) Live/dead images of HERS cells encapsulated in GelMA hydrogel on days 1, 4, and 7. BF: Bright field; Merge 1, merge of Live and Dead images; Merge 2, merge of live, dead, and BF images. (C) Quantitative analysis of cell viability, $^{***}P < 0.001$. HERS: Hertwig's epithelial root sheath, GelMA: Gelatin methacrylate.

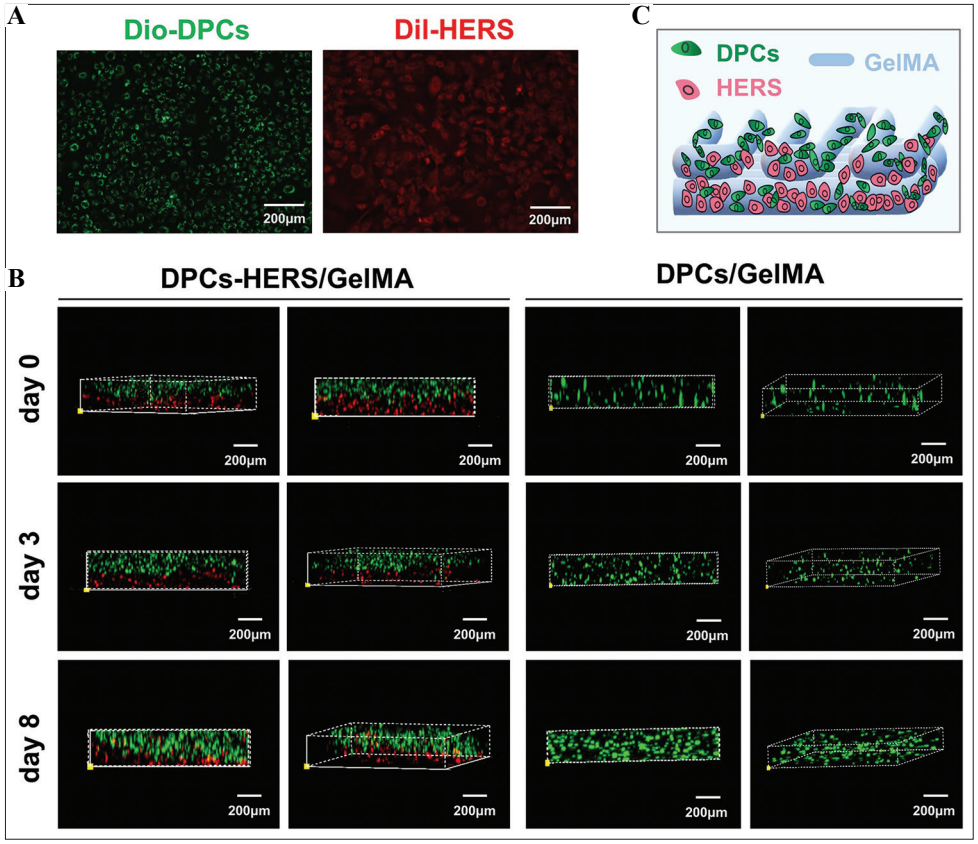

Figure 3. *In vitro* HERS-DPCs interaction. (A) DPCs and HERS cells were dyed by Dio and Dil cell-labeling solution separately. (B) Confocal images of cells/GelMA constructs after culture *in vitro* for 0, 3, and 8 days. In HERS-DPCs co-culture, these two kinds of cells migrated to each other, and the interface between HERS cells and DPCs was getting blurry on day 8. (C) Schema chart of migration of HERS cells and DPCs. HERS: Hertwig's epithelial root sheath, DPCs: Dental papilla cells, GelMA: Gelatin methacrylate.

had fewer and thinner fiber. The markers involved in this study include osteogenic-related markers (COL-I, OCN, and RUNX-2) and dentin marker like DSPP. COL-I, OCN, and RUNX-2 showed positive expression clearly in DPCs group and HERS+DPCs (3D) group while osteogenesis was also spotted in the 3D printed HERS+DPCs group (**Figure 5**). The HERS+DPCs (3D) group displayed more positive expression of DSPP than the HERS+DPCs (mixed) group.

4. Discussion

The serial interactions between epithelial cells and mesenchymal cells are crucial for tooth development and regeneration[35-37]. Studies have shown that the close contact between mesenchymal cells and basement membranes of epithelial cells mediated the differentiation of DPCs[38]. However, in the research of tooth regeneration, HERS tends to lose its epithelial characteristics through epithelial-mesenchymal transformation (EMT), thus losing the ability of inducing mesenchymal cells to differentiate[26,39,40]. The previously fabricated HERS spheroids differentiated or induced DPCs to form mineralized tissue both *in vitro* and *in vivo*[10]. HERS cells extracted from the tooth germ of neonatal rats in this experiment expressed both epithelial and mesenchymal markers, indicating that EMT had occurred in HERS cells (Passage 1) during this period (**Figure 2A, b-c**).

This experiment further explored the methods to promote the interaction between HERS cells and DPCs. We hypothesized that the 3D printed structure could construct a dimensional environment conducive to cell growth. GelMA has been used as the scaffold material of 3D printing in many studies for its physical and mechanical properties[32,41]. Barros *et al*. proposed a method for constructing the 3D skin model by using GelMA-based bioinks[25]. GelMA/alginate hydrogel loaded with human umbilical vein endothelial cells was printed on polyester porous membrane[41], and the construct was beneficial to both the diffusion of nutrients through forming internal vascular network and the interaction between dermal fibroblasts and endothelial cells. In this study, the high cell viability in 3D-printed constructs suggested that GelMA hydrogel had good biocompatibility (**Figure 2B and C and Figure S2**). In the *in vitro* experiment of HERS-DPCs interaction, compared to the 3D-printed DPCs/GelMA group, the two cells migrated to each other significantly after 8 days of co-culture (**Figure 3B**). The interface between HERS

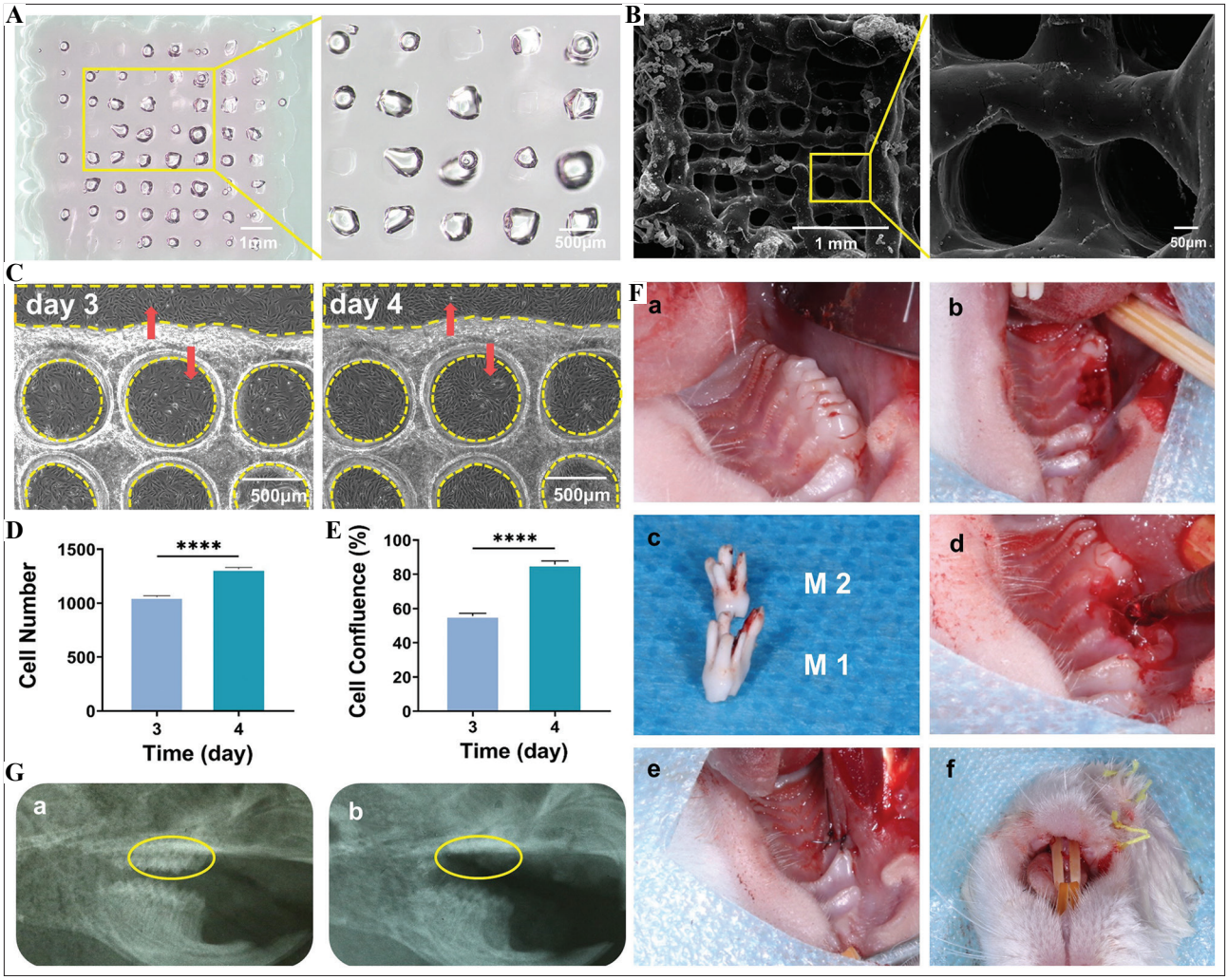

Figure 4. Microscopic observation and alveolar socket transplantation of printed construct. (A) Optical microscope images of 3D printed construct in culture medium. (B) SEM images of printed construct show the staggered grid structure. (C) Cells crawled out from the GelMA scaffold (red arrow) and proliferated since day 3. (D) Quantitative analysis of cell number on day 3 and day 4, $^{****}P < 0.0001$. (E) Quantitative analysis of cell confluence on day 3 and day 4，$^{****}P < 0.0001$. (F) The flow of animal experiments: (a) exposure of the operation area; (b) extraction of the first and second upper right molars; (c) M 1: The first molar extracted from the right maxilla, M 2: The second molar extracted from the right maxilla; (d) preparation of alveolar bone defect; (e) suture of the mucosa; and (f) suture of skin. (G) X-ray films of jaw bone before (a) and after (b) operation.

cells and DPCs was getting blurry, indicating that the 3D printing structure model of this experiment was conducive to the migration and growth of HERS cells and DPCs. We drew a schematic diagram to display the migration of the two kinds of cells vividly (**Figure 3C**).

Cell differentiation requires specific micro-environment induction[42-44]. The alveolar fossa model we constructed simulated the micro-environment for HERS cells and DPCs to proliferate and differentiate. The staggered grid design provided enough space for cell proliferation, and we found that massive cells encapsulated in GelMA crawled out of scaffolds on the 3rd day and proliferated rapidly (**Figure 4A-C**). In addition, the cell confluence increased from approximately 55% to 80% from day 3 to day 4 (**Figure 4E**). Therefore, the printed constructs were cultured *in vitro* for 4 days before transplanting into alveolar socket and then observed *in vivo* for 8 weeks. HE, Masson and immunohistochemical staining were applied to assess the osteogenesis. The osteogenesis of blank group and HERS group was not obvious. Significantly, DPCs group had positive expression of osteogenic markers, including COL-I, OCN, and RUNX-2[45-47]. This result may be explained by the fact that DPCs differentiated into osteoblasts to promote bone formation under the induction of micro-environment in alveolar fossa (**Figure 5**). Except for the expression of osteogenic markers, new bone formation also occurred in HERS+DPCs (3D bioprinting) group. It seems possible that these results were due to the induction of HERS cells in 3D culture environment. This micro-

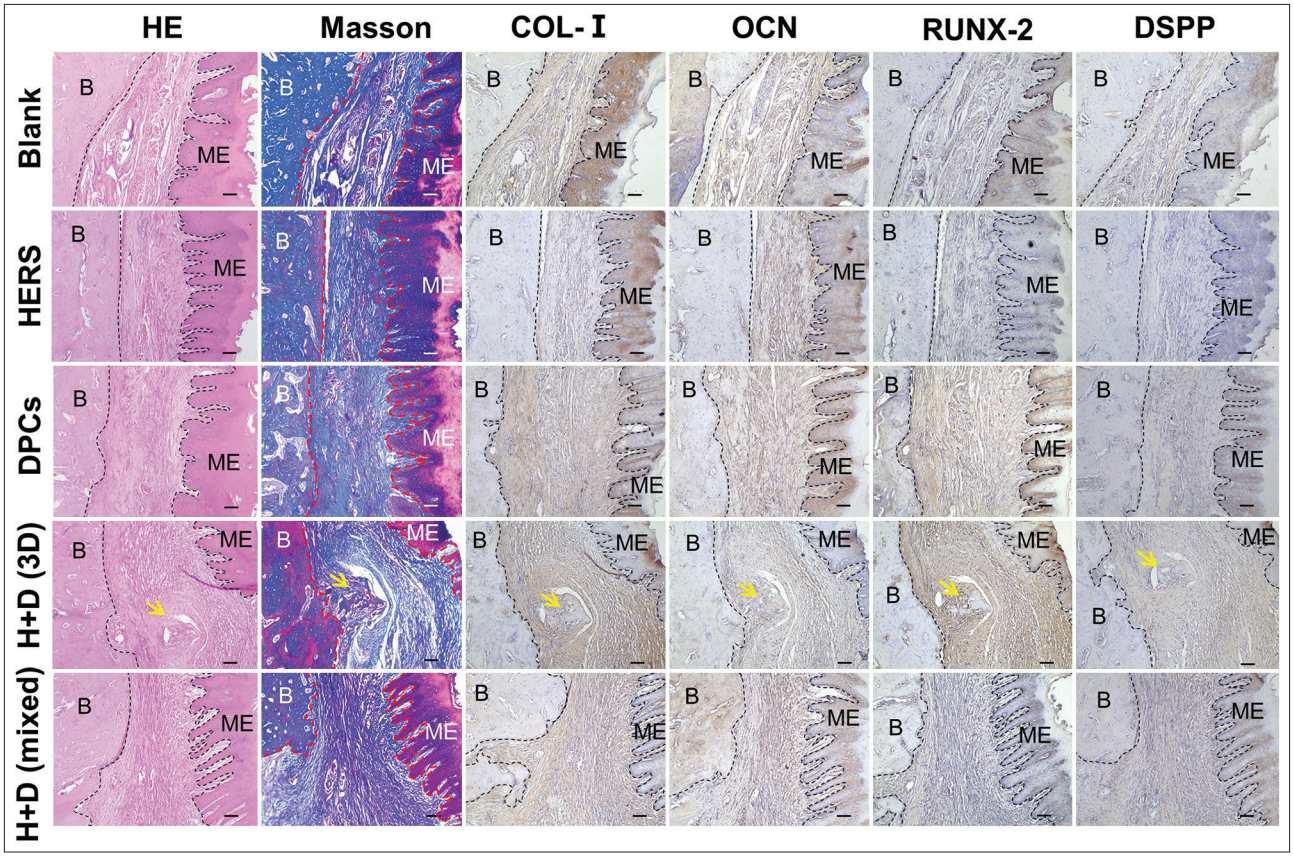

Figure 5. Hematoxylin and eosin staining, Masson staining and immunohistochemical evaluations of implantation in alveolar bone after 8 weeks. The groups were divided as blank, DPCs (3D bioprinting), HERS (3D bioprinting), HERS+DPCs (3D bioprinting) and HERS+DPCs (mixed). No implant was used to fill the alveolar bone defect in the blank group. HERS+DPCs (mixed) group mixed two cells in GelMA directly without 3D bioprinting. DPCs group had positive expression of osteogenic markers, including COL-I, OCN, and RUNX-2. Except for the expression of osteogenic markers, new bone formation (yellow arrow) also occurred in HERS+DPCs (3D bioprinting) group. Scale bars = 100 μm. B: Alveolar bone, ME: Mucosa epithelium, HERS: Hertwig's epithelial root sheath, DPCs: Dental papilla cells, GelMA: Gelatin methacrylate.

environment was conducive to DPCs differentiating into osteoblasts and bone repair in alveolar fossa. In addition, dentin marker DSPP was positively expressed in both 3D printing group and mixed group[47], indicating that there was no obvious relativity between the differentiation of DPCs and the scaffold structure. These results suggested that the construction of three-dimensional micro-environment for HERS-DPCs interaction by 3D printing is beneficial to the differentiation of DPCs. Although the mechanism of interactions between HERS cells and DPCs in GelMA scaffold remains unknown, our research on HERS-DPCs co-culture model through 3D bioprinting provides new insights into the EMI study and we will continue to investigate this issue in depth in the future.

5. Conclusion

The main goal of the current study is to investigate the feasibility of recombination of HERS cells and DPCs through 3D bioprinting. The results of cell viability and proliferation indicate that the printed GelMA scaffold could provide adequate conditions for cell activities. Besides, the constructed 3D HERS-DPCs co-culture model might simulate the micro-environment during tooth development *in vivo*, which was favorable for interactions between these two kinds of cells. Thus, the HERS-DPCs group shows better alveolar bone regeneration in SD rat models. This study certainly expanded our understanding of the strategy for dental EMI research.

Acknowledgments

The 3D printing of cell-laden GelMA constructs was carried out by Chengdu Renjitiancheng Biotechnology Co., Ltd. The authors wish to thank all staffs for their contributions to this study.

Funding

This study was supported by the National Natural Science Foundation of China (31971281), and Research and

Develop Program, West China Hospital of Stomatology, Sichuan University (RD-03-202106).

Conflict of interest

The authors declare no conflicts of interest.

Author contributions

H.T. performed the experiments and data analysis, and wrote the article. F.B. contributed in cell culture and animal experiments. G.C. designed the study and guided the experiments. Y.H. contributed in 3D bioprinting S.Z. and J.C. contributed in animal experiments. L.X. guided the experiments. X.Q. contributed in 3D bioprinting and revised the article. W.G. designed the study and revised the article. All authors have read and approved the manuscript.

References

1. Nanci A, editor, 2013, Development of the Tooth and its Supporting Tissues. In: Ten Cate's Oral Histology: Development, Structure, and Function. St. Louis, Missouri: Elsevier, Mosby. p70–71. https://doi.org/10.1016/B978-0-323-07846-7.00005-7
2. Zhang YD, Chen Z, Song YQ, *et al*., 2005, Making a Tooth: Growth Factors, Transcription Factors, and Stem Cells. *Cell Res*, 15:301–16. http://doi.org/10.1038/sj.cr.7290299
3. De Luca M, Aiuti A, Cossu G, *et al*., 2019, Advances in Stem Cell Research and Therapeutic Development. *Nat Cell Biol*, 21:801–11. http://doi.org/10.1038/s41556-019-0344-z
4. Ikeda E, Morita R, Nakao K, *et al*., 2009, Fully Functional Bioengineered Tooth Replacement as an Organ Replacement Therapy. *Proc Natl Acad Sci U S A*, 106:13475–80. http://doi.org/10.1073/pnas.0902944106
5. Nakao K, Morita R, Saji Y, *et al*., 2007, The Development of a Bioengineered Organ Germ Method. *Nat Methods*, 4:227–30. http://doi.org/10.1038/nmeth1012
6. Monteiro N, Smith EE, Angstadt S, *et al*., 2016, Dental Cell Sheet Biomimetic Tooth Bud Model. *Biomaterials*, 106:167–79. http://doi.org/10.1016/j.biomaterials.2016.08.024
7. Smith EE, Angstadt S, Monteiro N, *et al*., 2018, Bioengineered Tooth Buds Exhibit Features of Natural Tooth Buds. *J Dent Res*, 97:1144–51. http://doi.org/10.1177/0022034518779075
8. Nanci A, editor, 2013, Development of the Tooth and its Supporting Tissues. In: Ten Cate's Oral Histology: Development, Structure, and Function. St. Louis, Missouri: Elsevier, Mosby. p89–90. https://doi.org/10.1016/B978-0-323-07846-7.00005-7
9. Nanci A, editor, 2013, Periodontium. In: Ten Cate's Oral Histology: Development, Structure, and Function. St. Louis, Missouri: Elsevier, Mosby. p207. https://doi.org/10.1016/B978-0-323-07846-7.00009-4
10. Duan Y, Li X, Zhang S, *et al*., 2020, Therapeutic Potential of HERS Spheroids in Tooth Regeneration. *Theranostics*, 10:7409–21. http://doi.org/10.7150/thno.44782
11. Vijayavenkataraman S, Yan W, Lu WF, *et al*., 2018, 3D Bioprinting of Tissues and Organs for Regenerative Medicine. *Adv Drug Deliver Rev*, 132:296–332. http://doi.org/10.1016/j.addr.2018.07.004
12. Ji Y, Yang Q, Huang G, *et al*., 2019, Improved Resolution and Fidelity of Droplet-Based Bioprinting by Upward Ejection. *ACS Biomater Sci Eng*, 5:4112–21. http://doi.org/10.1021/acsbiomaterials.9b00400
13. Yang Q, Lian Q, Xu F, 2017, Perspective: Fabrication of integrated organ-on-a-chip via bioprinting. *Biomicrofluidics*, 11:31301. http://doi.org/10.1063/1.4982945
14. Qing H, Ji Y, Li W, *et al*., 2020, Microfluidic Printing of Three-Dimensional Graphene Electroactive Microfibrous Scaffolds. *ACS Appl Mater Interfaces*, 12:2049–58. http://doi.org/10.1021/acsami.9b17948
15. Yang Q, Gao B, Xu F, 2019, Recent Advances in 4D Bioprinting. *Biotechnol J*, 15:1900086. http://doi.org/10.1002/biot.201900086
16. Bordas SP, Balint DS, editors, 2021, Mechanics of Hydrogel-based Bioprinting: From 3D to 4D. In: Advances in Applied Mechanics. San Diego, CA: Elsevier. p285–318. https://doi.org/10.1016/bs.aams.2021.03.001
17. Gao B, Yang Q, Zhao X, *et al*., 2016, 4D Bioprinting for Biomedical Applications. *Trends Biotechnol*, 34:746–56. http://doi.org/10.1016/j.tibtech.2016.03.004
18. Zhou M, Lee BH, Tan LP, 2017, A Dual Crosslinking Strategy to Tailor Rheological Properties of Gelatin Methacryloyl. *Int J Bioprinting*, 3:3. http://doi.org/10.18063/IJB.2017.02.003
19. Ma Y, Xie L, Yang B, *et al*., 2018, Three-Dimensional Printing Biotechnology for the Regeneration of the Tooth and Tooth-supporting Tissues. *Biotechnol Bioeng*, 116:452–68. http://doi.org/10.1002/bit.26882
20. Yang T, Zhang Q, Xie L, *et al*., 2021, hDPSC-laden GelMA Microspheres Fabricated Using Electrostatic Microdroplet Method for Endodontic Regeneration. *Mater Sci Eng C*, 121:111850.

http://doi.org/10.1016/j.msec.2020.111850

21. Smith EE, Zhang W, Schiele NR, *et al*., 2017, Developing a Biomimetic Tooth Bud Model. *J Tissue Eng Regen Med*, 11:3326–36. http://doi.org/10.1002/term.2246
22. Khayat A, Monteiro N, Smith EE, *et al*., 2016, GelMA-Encapsulated hDPSCs and HUVECs for Dental Pulp Regeneration. *J Dent Res*, 96:192–9. http://doi.org/10.1177/0022034516682005
23. Murphy C, Kolan K, Li W, *et al*., 2017, 3D Bioprinting of Stem Cells and Polymer/Bioactive Glass Composite Scaffolds for Tissue Engineering. *Int J Bioprint*, 3:5. http://doi.org/10.18063/IJB.2017.01.005
24. Ma Y, Ji Y, Zhong T, *et al*., 2017, Bioprinting-Based PDLSC-ECM Screening for in Vivo Repair of Alveolar Bone Defect Using Cell-Laden, Injectable and Photocrosslinkable Hydrogels. *ACS Biomater Sci Eng*, 3:3534–45. http://doi.org/10.1021/acsbiomaterials.7b00601
25. Barros NR, Kim H, Gouidie MJ, *et al*., 2021, Biofabrication of Endothelial Cell, Dermal Fibroblast, and Multilayered Keratinocyte Layers for Skin Tissue Engineering. *Biofabrication*, 13:35030. http://doi.org/10.1088/1758-5090/aba503
26. Chen J, Chen G, Yan Z, *et al*., 2014, TGF-β1 and FGF2 Stimulate the Epithelial-Mesenchymal Transition of HERS Cells Through a MEK-Dependent Mechanism, *J Cell Physiol*, 229:1647–59. http://doi.org/10.1002/jcp.24610
27. Chen G, Sun W, Liang Y, *et al*., 2017, Maternal Diabetes Modulates Offspring Cell Proliferation and Apoptosis During Odontogenesis via the TLR4/NF-κB Signalling Pathway. *Cell Prolif*, 50:e12324. http://doi.org/10.1111/cpr.12324
28. Chen T, Liu Z, Sun W, *et al*., 2015, Inhibition of Ape1 Redox Activity Promotes Odonto/osteogenic Differentiation of Dental Papilla Cells. *Sci Rep*, 5:17483. http://doi.org/10.1038/srep17483
29. Li X, Zhang S, Zhang Z, *et al*., 2019, Development of Immortalized Hertwig's Epithelial Root Sheath Cell Lines for Cementum and Dentin Regeneration. *Stem Cell Res Ther*, 10:3. http://doi.org/10.1186/s13287-018-1106-8
30. Billiet T, Gevaert E, De Schryver T, *et al*., 2014, The 3D Printing of Gelatin Methacrylamide Cell-laden Tissue-engineered Constructs with High Cell Viability. *Biomaterials*, 35:49–62. http://doi.org/10.1016/j.biomaterials.2013.09.078
31. Laronda MM, Rutz AL, Xiao S, *et al*., 2017, A Bioprosthetic Ovary Created Using 3D Printed Microporous Scaffolds Restores Ovarian Function in Sterilized Mice. *Nat Commun*, 8:15261. http://doi.org/10.1038/ncomms15261
32. Jiang G, Li S, Yu K, *et al*., 2021, A 3D-printed PRP-GelMA Hydrogel Promotes Osteochondral Regeneration through M2 Macrophage Polarization in a Rabbit Model. *Acta Biomater*, 128:150–62. http://doi.org/10.1016/j.actbio.2021.04.010
33. Ren J, Wang H, Tran K, *et al*., 2015, Human Bone Marrow Stromal Cell Confluence: Effects on Cell Characteristics and Methods of Assessment. *Cytotherapy*, 17:897–911. http://doi.org/10.1016/j.jcyt.2015.03.607
34. Odeleye AO, Castillo-Avila S, Boon M, *et al*., 2017, Development of an Optical System for the Non-invasive Tracking of Stem Cell Growth on Microcarriers. *Biotechnol Bioeng*, 114:2032–42. http://doi.org/10.1002/bit.26328
35. Honda MJ, Tsuchiya S, Sumita Y, *et al*., 2007, The Sequential Seeding of Epithelial and Mesenchymal Cells for Tissue-engineered Tooth Regeneration. *Biomaterials*, 28:680–9. http://doi.org/10.1016/j.biomaterials.2006.09.039
36. Thesleff I, Hurmerinta K, 1981, Tissue Interactions in Tooth Development. *Differentiation* (*London*), 18:75. https://doi.org/10.1111/j.1432-0436.1981.tb01107.x
37. Slavkin HC, Snead ML, Zeichner-David M, *et al*., 1984, Concepts of Epithelial-mesenchymal Interactions during Development: Tooth and Lung Organogenesis. *J Cell Biochem*, 26:117–25. http://doi.org/10.1002/jcb.240260207
38. Thesleff I, Lehtonen E, Saxen L, 1978, Basement Membrane Formation in Transfilter Tooth Culture and its Relation to Odontoblast Differentiation. *Differentiation*, 10:71–9. http://doi.org/10.1111/j.1432-0436.1978.tb00948.x
39. Zeichner-David M, Oishi K, Su Z, *et al*., 2003, Role of Hertwig's Epithelial Root Sheath Cells in Tooth Root Development. *Dev Dyn*, 228:651–63. http://doi.org/10.1002/dvdy.10404
40. Sonoyama W, Seo BM, Yamaza T, *et al*., 2007, Human Hertwig's Epithelial Root Sheath Cells Play Crucial Roles in Cementum Formation. *J Dent Res*, 86:594–9. http://doi.org/10.1177/154405910708600703
41. Xie M, Zheng Y, Gao Q, *et al*., 2021, Facile 3D Cell Culture Protocol Based on Photocurable Hydrogels. *Biodes Manuf*, 4:149–53. http://doi.org/10.1007/s42242-020-00096-2
42. Yelick PC, Sharpe PT, 2019, Tooth Bioengineering and Regenerative Dentistry. *J Dent Res*, 98:1173–82.

http://doi.org/10.1177/0022034519861903

43. Ono M, Oshima M, Ogawa M, *et al*., 2017, Practical Whole-tooth Restoration Utilizing Autologous Bioengineered Tooth Germ Transplantation in a Postnatal Canine Model. *Sci Rep*, 7:44522.
http://doi.org/10.1038/srep44522

44. Li J, Parada C, Chai Y, 2017, Cellular and Molecular Mechanisms of Tooth Root Development. *Development*, 144:374–84.
http://doi.org/10.1242/dev.137216

45. Aubin JE, Liu F, Malaval L, *et al*., 1995, Osteoblast and Chondroblast Differentiation. *Bone*, 17 Suppl2:77S–83.
http://doi.org/10.1016/8756-3282(95)00183-e

46. Kim S, Turnbull J, Guimond S, 2011, Extracellular Matrix and Cell Signalling: The Dynamic Cooperation of Integrin, Proteoglycan and Growth Factor Receptor. *J Endocrinol*, 209:139–51.
http://doi.org/10.1530/JOE-10-0377

47. Li W, Chen L, Chen Z, *et al*., 2017, Dentin Sialoprotein Facilitates Dental Mesenchymal Cell Differentiation and Dentin Formation. *Sci Rep*, 7:300.
http://doi.org/10.1038/s41598-017-00339-w

Publisher's note